Detection and Modeling of Non-Tidal Oceanic Effects on the Earth's Rotation Rate

Steven L. Marcus, Yi Chao, Jean O. Dickey, and Pascal Gegout
Jet Propulsion Laboratory, California Institute of Technology
4800 Oak Grove Drive
Pasadéna CA 91109

May 1998

Submitted to *Science*

Abstract

Sub-decadal changes in the Earth's rotation rate, and hence in the length-of-day (LOD), are largely controlled by variations in atmospheric angular momentum. Here, we use results from two oceanic general circulation models (OGCMs), forced by observed surface wind stress and heat flux for the years 1992-1994, to demonstrate that ocean current and mass distribution changes also induce detectable LOD variations. The close similarity of the axial oceanic angular momentum (OAM) results from two independent OGCMs, and their significant coherence with space geodetic determinations of LOD, demonstrate that global ocean models can successfully capture the large-scale circulation changes which drive OAM variability on seasonal and shorter time scales.

Detection and Modeling of Non-Tidal Oceanic Effects on the Earth's Rotation Rate

Changes in the rotation rate of the solid Earth (i.e. its crust and mantle), commonly expressed as variations in the length-of-day (LOD), have magnitudes ranging up to about a millisecond on sub-decadal time scales (*1*). The Earth as a whole conserves its angular momentum (with the exception of tidal torques); seasonal LOD variations, in particular, have been shown to arise largely from concomitant changes in atmospheric angular momentum (AAM) carried by zonal (i.e. west-to-east) winds (*2*). Indeed, significant coherence between time series of LOD and AAM has been found to extend to periods as short as about ten days, with loss of coherence at higher frequencies resulting from declining signal-to-noise ratios in both data types (*3*). Remaining discrepancies in the axial budget, however, indicate that other reservoirs also store and release appreciable quantities of angular momentum on these time scales; in addition to yielding a more complete picture of the rotational dynamics of the Earth system, their eludication will provide further insight into the interactions among its components.

With the advent of satellite-based altimetry and ocean general circulation models (OGCMs), the oceans' role in the Earth system has recently become a topic of heightened interest. In this study we focus on the contribution of the oceans to the Earth's axial angular momentum budget: in particular, we wish to determine (i) whether a significant non-tidal oceanic signal can be detected in geodetic LOD series, and (ii) the potential contribution of oceanic angular momentum (OAM) towards closing the global budget on seasonal and shorter time scales. Since the three-dimensional observational data needed to compute OAM directly are not available, we use OGCM simulations as a proxy for our analysis. Evaluation of the quality of simulated OAM series through comparisons with independent geodetic and atmospheric data can provide a valuable check on the realism of the OGCMs which produce them; conversely, model-derived OAM estimates may be used to constrain potential contributions from other angular momentum reservoirs, such as changes in terrestrial and atmospheric water storage, to the global budget.

In order to assess the robustness of the simulated large-scale features which account for OAM variability, we consider results from two OGCMs whose dynamical formulations differ considerably: the Modular Ocean Model (*4*) (MOM), based on earlier multi-level models developed at the Geophysical Fluid Dynamics Laboratory (*5*), and a multi-layer model based on an early version of the Miami Isopycnal Coordinate Ocean Model (MICOM) (*6*). Both MOM and MICOM are based on the primitive equations of fluid flow that use the Boussinesq and hydrostatic approximations. The major differences between the two models are (i) vertical coordinate systems: MOM uses geometrical depth beneath a rigid lid, while MICOM employs a density-based coordinate with a freely-varying surface height; and (ii) the treatment of the surface mixed layer: MOM uses a Richardson-number scheme (*7*), while MICOM employs the Kraus-Turner mixed layer model (*8*). Both models have a horizontal resolution of 2° long x 1° lat and comparable vertical resolution (22 levels vs. 12 layers).

The OGCMs were spun up for ten years starting from climatological temperature and salinity distributions (*9*), forced with climatological monthly wind stress (*10*) and sea surface temperature and salinity (*9*). After ten years of spinup, the models were driven with surface wind stress derived from the daily National Center for Environmental Prediction (NCEP) 1000-mb analysis from 1 January 1992 to 15 December 1994, and heat flux computed using the bulk formulation described in ref. (*11*); the first 45 days were excluded from the analysis to eliminate transient effects. Pressure forcing by the atmosphere was not included (*12*).

Fig. 1a shows the contribution to OAM variations calculated from the zonal oceanic currents simulated by each model. These terms represent changes in the relative axial angular momentum of the oceans, and are expressed in units of equivalent LOD. Both models are characterized by a net west-to-east flow which sequesters positive angular momentum and slows the rotation of the solid Earth, giving rise to a mean positive LOD forcing of approximately 100 microseconds (μs); for comparison the atmosphere superrotates at a mean velocity of roughly 7 ms^{-1} and contributes about 2.5 milliseconds (ms) to the average LOD -- cf. Fig. 2a. Note that both current terms are characterized by drifts which are approximately linear in time but opposite in sign; removal of these trends, which reflect the incomplete equilibration of the deeper oceanic layers during the spinup phase, leaves relative OAM variations which are quite similar between the MICOM and MOM simulations (not shown), with rms magnitude 12.7 and 14.5 μs, respectively.

Because of the background planetary rotation, changes in the oceans' moment of inertia also induce OAM variations (their effect on the relative angular momentum is orders of magnitude smaller and is neglected). Changes in the planetary terms for the two models (Fig. 1b) again show long-term trends of opposite sign, although these are not linear and are much larger than the corresponding trends for the relative OAM. Due to the use of the Boussinesq approximation in the governing equations, both models conserve volume rather than mass; the OAM represented by the consequently "missing" sea level variations (dashed lines -- cf. ref. *13*) closely resembles the planetary OAM trend generated by each model. The removal of linear trends and the effects of mass non-conservation yields time series of planetary OAM (not shown) that are very similar between the MOM and MICOM results; their respective rms magnitudes are 21.2 and 22.5 μs, nearly twice that of the relative OAM variation.

The total OAM variations obtained by adding the latter planetary OAM variations (cf. Fig. 1b) and the linearly detrended relative OAM variations (cf. Fig. 1a) are surprisingly alike over the nearly three years simulated by the two models (Fig. 1c), given their distinct dynamical formulations and the differences in long-term trends following spinup. This excellent agreement between their axial OAM results increases our confidence in the robustness of the models' simulation of the circulation features that contribute to the axial OAM, i.e., the large-scale current systems and mass distribution (*14*). In what follows, we seek to evaluate the accuracy of these robust results through comparisons with independent geodetic and atmospheric estimates of LOD excitation during the period of the OGCM simulations.

An LOD time series, sampled at daily intervals from the Kalman-filtered SPACE96 calculation (*15*), is shown in Fig. 2a; since the data are defined with respect to an arbitrary reference value for the standard LOD, the vertical offset has no physical significance. The effects of tidal forcing on both the solid Earth and oceans has been removed from this series (*16*). Also shown is the estimated LOD forcing due to atmospheric winds integrated from 1000 hPa to 0.3 hPa; values below 10 hPa were computed as the averages of global wind analyses provided by the ECMWF, JMA, and the NCEP-NCAR reanalysis campaign (*17*), while those above 10 hPa were obtained from the BADC (*18*). Both the geodetic and atmospheric series contain a strong seasonal signal; higher-frequency variability is also clearly shared by the two time series. For the atmosphere, variations in global angular momentum arising from moment-of-inertia changes are roughly an order of magnitude smaller than those driven by wind fluctuations (*1*); the axial moment of the atmosphere also depends on changes in its water vapor content, and this contribution will be addressed in a future study.

In a closed two-component system consisting of the solid Earth and atmosphere the combined angular momentum would be constant, and this would be reflected by identical (although offset) shapes of the AAM and LOD series plotted here. To the extent that the estimates of both quantities in Fig. 2a are accurate and complete, therefore, the nonzero residual variation shown in Fig. 2b (note the difference in vertical scale) implies the participation of additional angular momentum reservoirs in the global budget. Variations in core motions are believed to be responsible for observed century-scale excursions of up to several ms in LOD (*1*). As the core is only weakly coupled to the mantle on the shorter time scales considered here (*19*), we account for its effect by removing a least-squares-fit quadratic trend from the LOD-AAM variation. The residual LOD-AAM signal is shown in Fig. 2c; it represents the "missing" part of the Earth's axial angular momentum budget, and has an rms magnitude of 60.5 μs.

The total OAM series generated by the MICOM and MOM models (Fig. 1c) have rms magnitudes of 30.7 and 30.5 μs, respectively, and thus potentially represent about half of the residual LOD variation. The MICOM series, shown in Fig. 2c with a quadratic background removed, bears a striking similarity to the LOD-AAM residual (correlation coefficient = 0.77), and explains 42% of its variance; comparison of the MOM series with the LOD-AAM residual (not shown) yields slightly lower results for the correlation coefficient (0.72) and explained variance (34%). The correlation coefficients from both models, in particular, are highly significant (at approximately the 3σ level), and clearly demonstrate the detection of a non-tidal oceanic signal in the Earth's rotation rate.

Further insight into the oceans' effect on Earth rotation may be gained by comparing geodetic, atmospheric and oceanic signals in the frequency domain. LOD spectra (not shown) contain strong seasonal peaks, with amplitudes varying in the range 0.3 - 0.4 ms (*20*). These peaks are still evident in our LOD data following removal of the wind excitation in the 1000 - 10 hPa layer (Fig. 3a), although the amplitude has been reduced by an order of magnitude. As emphasized in ref. (*2*), the winds above the 10 hPa level (carrying ~ 1% of the total atmospheric mass) make a disproportionately large contribution to the seasonal AAM cycle; removal of the excitation due to BADC winds (10 - 0.3 hPa) gives a particularly strong reduction in our results at the annual period, where the residual LOD amplitude is now comparable to that of the low-frequency background.

The OAM time series generated by the OGCM runs also contain seasonal rotation signals, as evidenced by the pronounced decrease in the residual LOD amplitudes (red lines in Fig. 3a) at the first two annual harmonics. Removal of the oceanic excitation simulated by both models, in fact, produces local amplitude minima within a bandwidth of the annual frequency, suggesting that the oceans play a significant role in the axial angular momentum budget on that timescale (*21*). At the semiannual period, both the 10 - 0.3 hPa winds and the oceanic excitation reduce the LOD residual, with the latter having a greater impact. It is interesting to note, moreover, that the upper-atmospheric data apparently contain little of the LOD signal at subseasonal periods, since their incorporation into the atmospheric excitation fails to reduce the spectral amplitude relative to the 1000 - 10 hPa residual in that range. The oceanic excitation from both models, by contrast, consistently lowers the LOD residuals at frequencies up to about $(25\ \text{day})^{-1}$.

Further evidence for the presence of a rotational signal in the OGCM results can be obtained from their effect on the coherence of LOD with its excitation sources. The atmospheric data sets used in our study produce coherence with LOD significant at the 95% level for all frequencies up to $(10\ \text{day})^{-1}$; note, however, that the addition of the 10 - 0.3 hPa winds to the 1000 - 10 hPa data yields no consistent improvement at the subseasonal frequencies plotted here (Fig. 3b, black lines). By contrast, addition of the OAM data from both models to the atmospheric excitation consistently increases the coherence with LOD at frequencies up to $(25\ \text{day})^{-1}$, and generally improves the results up to $(15\ \text{day})^{-1}$. At higher frequencies the effects of incorporating the OAM series are mixed, with the MICOM values generally giving better results; in particular, the combined AAM and MICOM excitation maintains coherence with LOD significant at the 99% level for all frequencies up to $(10\ \text{day})^{-1}$.

In summary, we have seen that OGCMs can realistically simulate the large-scale circulation features which drive axial OAM variability on seasonal and shorter time scales. The robustness of our results was confirmed by intercomparison of simulations from a multi-level (MOM) and multi-layer (MICOM) model using depth- and density-based vertical coordinates, respectively, and by evaluation of the impact of the computed oceanic excitation on observed variations in the Earth's rotation rate (*22*). The superior results obtained with MICOM at high frequency appear to be due to its isopycnal formulation and better treatment of the mixed layer (*23*). The future use of satellite altimetry and other complementary data types in constraining OGCMs will further increase our confidence in their simulations and therefore provide an even more accurate closure to the Earth's angular momentum budget.

REFERENCES AND NOTES

1. R. Hide and J. O. Dickey, *Science* **253**, 629 (1991); R. D. Rosen, *Surv. Geophys.* **14**, 1 (1993).
2. R. D. Rosen and D. A. Salstein, *Geophys. Res. Lett.* **18**, 1925 (1991).
3. J. O. Dickey, S. L. Marcus, J. A. Steppe, R. Hide, *Science* **255**, 321 (1992).
4. R. Pacanowski, K. Dixon, A. Rosati, "Modular ocean model users' guide," (Geophys. Fluid Dyn. Lab., NOAA, Princeton, N.J., 1991).
5. K. Bryan, *J. Comput. Phys.* **4**, 347 (1969); M. D. Cox, "A primitive equation, three-dimensional model of the ocean," *GFDL Ocean Group Tech. Rept. No. 1* (1984).

6. R. Bleck, H. P. Hanson, D. M. Hu, E. B. Kraus, *J. Phys. Ocean.* **19**, 1417 (1989); R. Bleck, C. Rooth, D. M. Hu, L. T. Smith, *J. Phys. Ocean.* **22**, 1486 (1992); D. M. Hu, *J. Phys. Ocean.* **27**, 96 (1997)

7. R. Pacanowski and S. G. H. Philander, *J. Phys. Ocean.* **11**, 1443 (1981).

8. E. B. Kraus and J. S. Turner, *Tellus* **19**, 98 (1967).

9. S. Levitus, *Climatological Atlas of the World Ocean* (NOAA Professional Paper No. 13, 173 pp., U.S. Govt. Print. Off., Washington, D.C., 1982).

10. S. Hellerman and M. Rosenstein, *J. Phys. Ocean.* **13**, 1903 (1983).

11. Y. Chao and L.-L. Fu, *J. Geophys. Res.* **100**, 24965 (1995).

12. On time scales greater than about ten days the ocean responds to atmospheric loading as an "inverted barometer", so that the total mass in a vertical column, and hence the combined moment of inertia of the ocean and overlying atmosphere, is not affected. For further details, see R. M. Ponte, *Geophys. J. Int.* **130**, 469 (1997).

13. J. Greatbach, *J. Geophys. Res.* **99**, 12767 (1994).

14. J. C. McWilliams, *Ann Rev. Fluid Mech.*, **28**, 215 (1996); for a general discussion of Earth rotation excitation by geophysical fluids see R. T. H. Barnes, R. Hide, A. A. White, C. A. Wison, *Proc. R. Soc. London, Ser. A.* **387**, 31 (1983).

15. R. S. Gross, in *1996 IERS Annual Report* (Observatoire de Paris, France, 1997, pp. II29).

16. S. D. Desai, Ph.D. Thesis, University of Colorado (1996).

17. AAM values were provided by the Sub-Bureau for Atmospheric Angular Momentum of the International Earth Rotation Service (D. A. Salstein, D. M. Kann, A. J. Miller, R. D. Rosen, *Bull. Am. Meteorol. Soc.* **74**, 67 (1993)), based on operational analyses from the European Centre for Medium-Range Weather Forecasts (ECMWF) and the Japanese Meteorological Agency (JMA). Data from the National Center for Environmental Prediction (NCEP) / National Center for Atmospheric Research (NCAR) 40-Year Reanalysis Project were used to calculate the NCEP AAM series (see D. A.

Salstein and R. D. Rosen, *7th Conf. on Climate Variations*, American Meteorological Society, Boston, MA, 344 (1997)).

18. AAM values above 10 hPa were computed from gridded wind data taken from the U.K. Meteorological Office's (UKMO's) Assimilated Data for UARS files and provided by the British Atmospheric Data Centre (BADC). For details, see R. Swinbank and A. O'Neill, *Mon. Wea. Rev.* **122**, 686 (1994).

19. R. Hide, in *Dynamics of Earth's Deep Interior and Earth Rotation*, J.-L. Le Mouel, D. E. Smylie, T. Herring, Eds. (Geophysical Monograph 72, American Geophysical Union, 1993), pp. 109-112.

20. R. S. Gross, S. L. Marcus, T. M. Eubanks, J. O. Dickey, C. L. Keppenne, *Geophys. Res. Lett.* **23**, 3373 (1996).

21. R. M. Ponte and R. D. Rosen, *J. Phys. Ocean.* **24**, 1966 (1994); F. O. Bryan, *Dyn. Atmos. Oceans* **25**, 191 (1997). Both of these studies found sizable annual signals in one-year samples of OAM taken from OGCM runs forced by monthly mean climatological winds; however, no comparisons using synoptic geodetic or atmospheric data were made.

22. For a recent discussion of oceanic effects on polar motion at seasonal and shorter time scales see R. M. Ponte, D. Stammer, J. Marshall, *Nature* **391**, 476 (1998).

23. D. Hu and Y. Chao, *Mon. Wea. Rev.*, in press.

24. We thank M. Ghil, R. Gross and R. Hide for useful comments on the manuscript. We are very grateful to D. Hu, who helped with the MICOM integration, and to D. Dong for the OAM calculation. Computations were performed on the Cray J-90 computer through the JPL Supercomputing project. The work of the authors was carried out by the Jet Propulsion Laboratory, California Institute of Technology, under contract with the National Aeronautics and Space Administration.

Figure Captions

Fig. 1. LOD excitation computed from the OGCM results. Both models were forced with surface wind stress and heat flux computed from daily NCEP analyses; pressure forcing by the atmosphere was not considered. (**A**) Relative oceanic angular momentum (OAM) contained in zonal currents (solid lines); positive LOD forcing corresponds to a net west-to-east flow. The dashed lines indicate least-squares-fit linear trends for each model series. (**B**) Planetary OAM changes for the two OGCM simulations (solid); the time mean has been removed from each series. Dashed lines indicate the change due to variations in the total mass content of each model (see text for details). (**C**) Sum of relative and planetary OAM changes for each model, following removal of linear trends and the effects of mass non-conservation.

Fig. 2. (**A**) Comparison of observed LOD with atmospheric forcing, computed from zonal winds integrated from 1000 to 0.3 hPa. (**B**) The difference between the LOD and AAM curves plotted in frame (A), compared with a least-squares-fit second-order polynomial used to represent the effects of core-mantle coupling. (**C**) The difference between the LOD-AAM and quadratic terms plotted in frame (B), compared with the total OAM computed from the MICOM simulation.

Fig. 3. (**A**) Amplitude spectra of LOD residuals after subtraction of atmospheric and oceanic excitation. AAM was computed from winds supplied by the ECMWF and JMA analysis and NCEP reanalysis campaigns for the 1000 - 10 hPa layer, and from BADC winds for the 10 - 0.3 hPa layer; the full (1000 - 0.3 hPa) AAM was used in combination with the OAM computed from the MOM and MICOM results. Spectral bandwidth is given by the width of the green bars, which are centered on the abscissa at the annual and semiannual frequencies. (**B**) Coherence squared of LOD with atmospheric and combined atmopheric and oceanic excitation sources (note difference in the frequency scale).

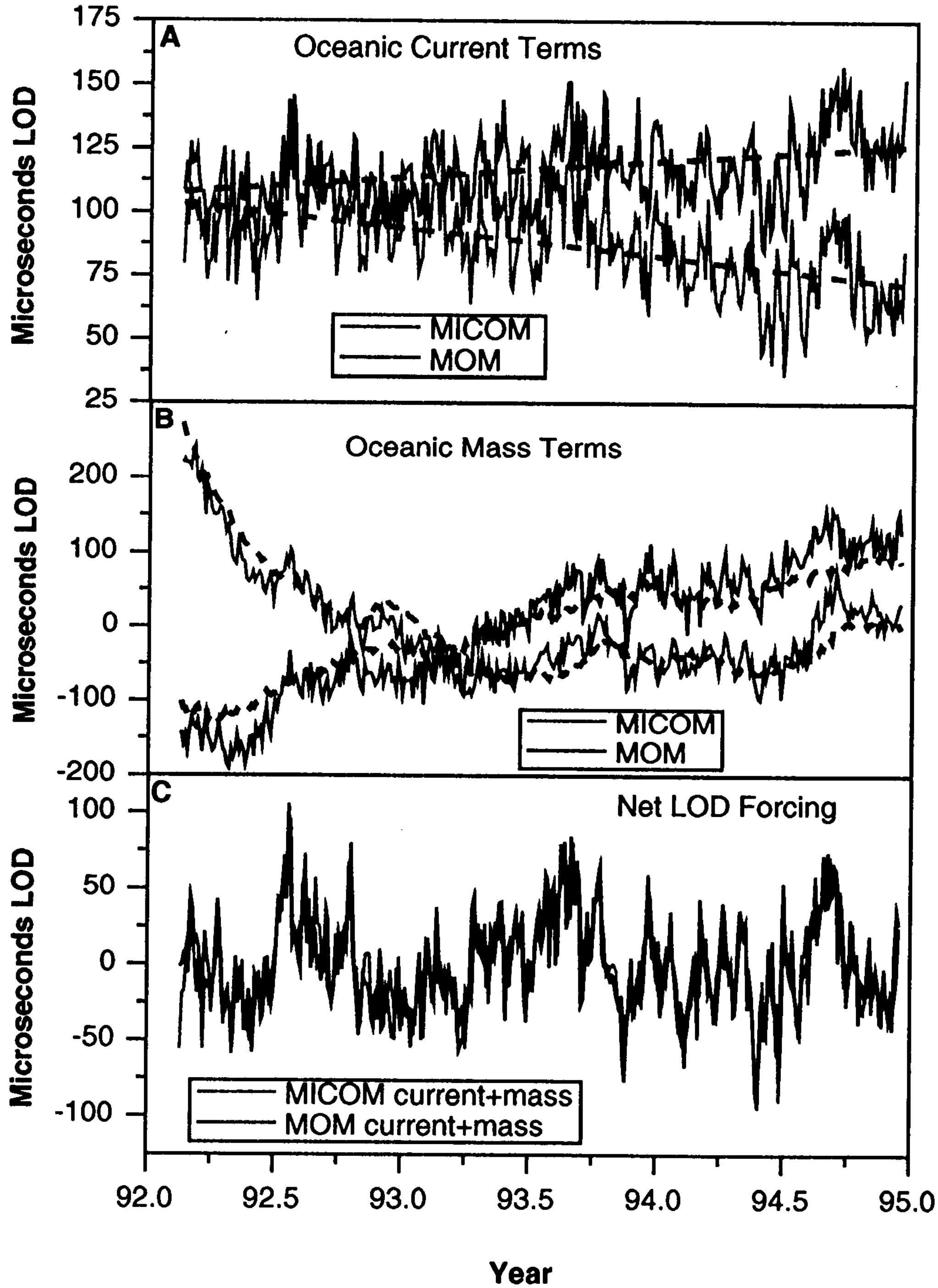
175
150
125
100
75
50
25
A
Oceanic Current Terms
MICOM
MOM
Microseconds LOD
B
Oceanic Mass Terms
200
100
0
-100
-200
MICOM
MOM
Microseconds LOD
C
Net LOD Forcing
100
50
0
-50
-100
MICOM current+mass
MOM current+mass
Microseconds LOD
92.0
92.5
93.0
93.5
94.0
94.5
95.0
Year

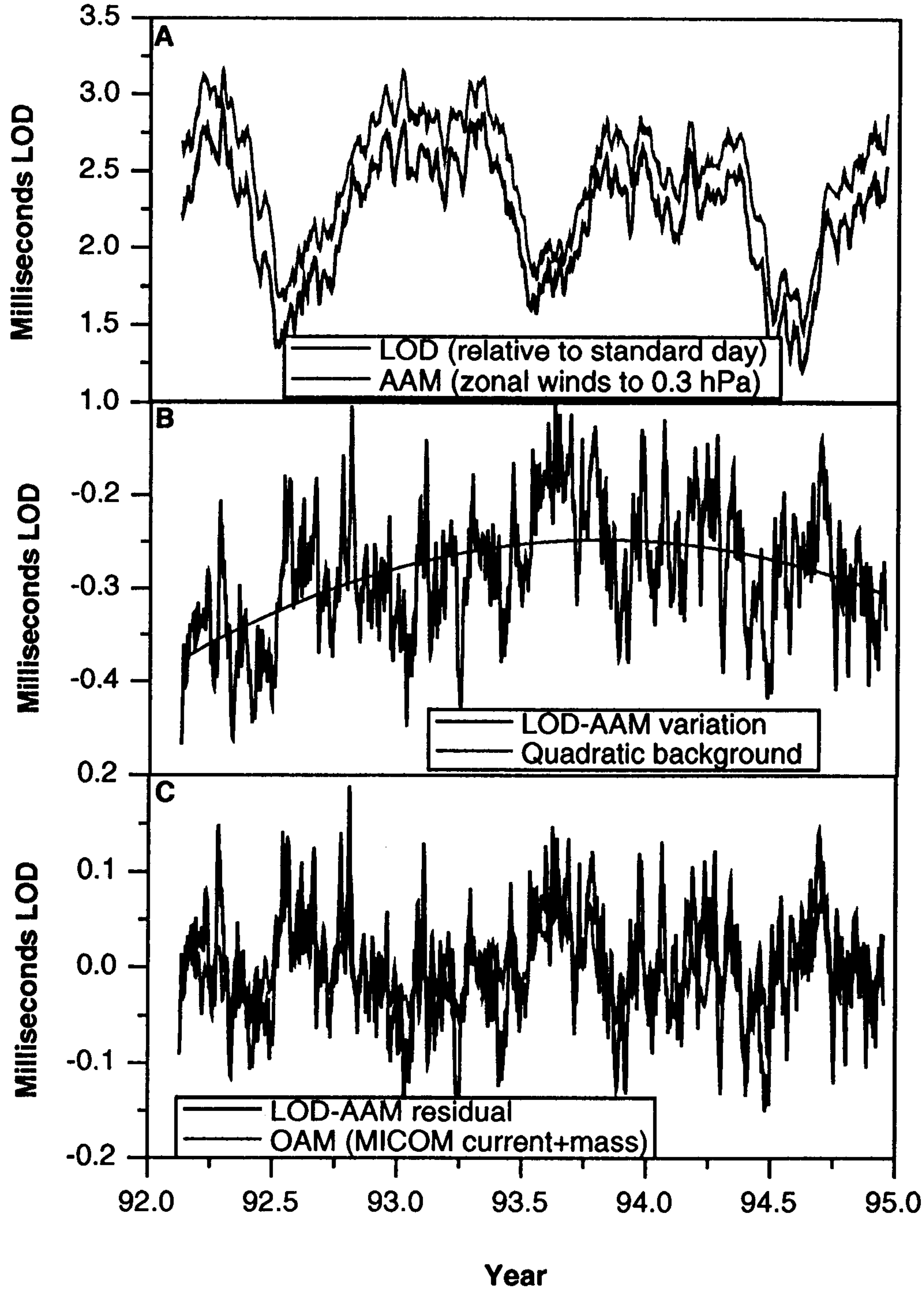

A
B
C
Milliseconds LOD
3.5
3.0
2.5
2.0
1.5
1.0
-0.2
-0.3
-0.4
0.2
0.1
0.0
-0.1
-0.2
LOD (relative to standard day)
AAM (zonal winds to 0.3 hPa)
LOD-AAM variation
Quadratic background
LOD-AAM residual
OAM (MICOM current+mass)
92.0
92.5
93.0
93.5
94.0
94.5
95.0
Year